Proceeding of the 2004 American Control Conference
Boston, Massachusetts June 30 - July 2, 2004

Control of Homogeneous Charge Compression Ignition (HCCI) Engine Dynamics

Johan Bengtsson†, Petter Strandh‡, Rolf Johansson†, Per Tunestål‡ and Bengt Johansson‡
† Dept. Automatic Control, Lund University, PO Box 118, SE 221 00 Lund, Sweden
‡ Div. Combustion Engines, Lund University, PO Box 118, SE-211 00, Lund, Sweden
Email: Johan.Bengtsson@control.lth.se

Abstract— **The Homogeneous Charge Compression Ignition (HCCI) combustion concept lacks direct ignition timing control, instead the auto ignition depends on the operating condition. Since auto ignition of a homogeneous mixture is very sensitive to operating conditions, a fast combustion timing control is necessary for reliable operation. Hence, feedback is needed and the crank angle of 50% burnt (CA50) has proved to be a reliable feedback indicator of on-going combustion in practice. CA50 or other methods for detecting on-going cylinder pressure used in the feedback control of a HCCI engine all rely on pressure sensors. This paper presents a new candidate for control of HCCI engine by using the electronic conductive properties in the reaction zone. This phenomenon is called ion current. This paper perform combustion timing control based on ion current and compare it with control based on pressure sensor. The combustion timing control is performed on cycle-to-cycle basis and the engine is a one-cylinder version of a heavy duty engine equipped with a port injection system using dual fuels.**

I. Introduction

One challenge with Homogeneous Charge Compression Ignition (HCCI) engines is the need for good timing control of the combustion. The HCCI engine differs from spark ignition engines and compression ignition engines, since it can only run in open-loop at low load. The main advantages of the HCCI engine are the very low NOx exhaust emissions and fairly high efficiency, close to that of compression ignition engines. Autoignition of a homogeneous mixture is sensitive to operating conditions, for example, even small variations of the load can change the timing from over-advanced to over-retarded combustion. As the ignition timing sets the performance limitation of the load control, a fast combustion timing control is necessary for reliable operation and to this purpose feedback is needed. Requirements for a practical and useful feedback for the timing of combustion are that it is accurate, stable and feasible for real-time control. With HCCI combustion, the cycle-to-cycle variations are smaller than with Spark Ignition (SI) combustion, but even so it is desirable to be able to perform cycle-to-cycle control of the timing of combustion. In practice, the crank angle of 50% burnt fuel (CA50) has proved to be a reliable indicator of on-going cylinder combustion in practice [3]. CA50 monitoring or other methods for monitor on-going combustion for feedback control of an HCCI engine all rely on pressure sensors. These sensors are expensive. One candidate to replace pressure sensors is using the electronic conductive properties for the reaction zone. This phenomenon is called ion current for which no expensive sensor is needed [4]. The basic principle of ion current sensing is that a voltage is applied over an electrode gap inserted into the actual gas volume (combustion chamber). In a non reacting charge, no ion current through the gap will be present. In a reacting (burning) charge, however, ions that carry an electrical current will be present. This means that the ion current reflects the conditions in the gas volume. In SI engines it is today used in production for misfire and knock detection [4]. The common belief so far has been that ion current levels are not measurable for the highly diluted HCCI combustion. However, a recent study shows that it is not the dilution level in itself but the actual fuel/air equivalence ratio which is an important factor for the signal level [1], [5]. Today there exist several means to control the combustion timing for an HCCI engine, for example, dual fuel, variable compression ratio, inlet temperature and variable valve timing. In this paper, an experimental set-up with dual fuels was used. Pressure-based CA50 we denote as $\alpha_{50,p}$ and corresponding based on ion current as $\alpha_{50,ion}$. The purpose of this paper was to demonstrate that closed-loop control based on ion current measurements works and to compare its performance with closed-loop control based on pressure measurements.

II. Experimental set-up

A. Engine system

The control performance comparison between ion current and pressure measurements were performed on a modified single cylinder version of a Volvo heavy duty engine TD100 (Table I). The engine was fitted with a spacer that had 6 evenly spaced radial 14mm fittings, which accommodated modified spark plugs. The only modification of the spark plugs was the removal of the side electrode. A cylinder pressure transducer was fitted to the engine for control and monitoring. Various ion current measurement points were tried, the one with the highest signal being used for control. The engine was fitted with an inlet air heater and it was operated with natural aspiration (Fig. 1). To control engine load and combustion phasing, the engine was fueled with dual fuels (iso-octane and n-heptane). The dual fuels give RON ratings from 0 up to 100. Engine speed was governed

0-7803-8335-4/04/$17.00 ©2004 AACC

TABLE I

SINGLE CYLINDER ENGINE SPECIFICATIONS.

Displaced Volume	1600 cm^3
Bore	120.65 mm
Stroke	140 mm
Connecting Rod Length	260 mm
Number of Valves	2
Compression Ratio	15.5:1
Fuel Supply	port fuel injection

by an electrical motor with the capability for both braking and motoring.

B. Control system

The engine was controlled by a combined data acquisition and engine control system. The engine control system ran on a standard PC with GNU/Linux operating system, resulting in a flexible platform for development of customized control systems with good soft real-time properties. All data coming from various sensors around the engine were collected in the main control program (Fig. 1). These data included various temperatures and pressures collected via a data logger, sampling at low sampling rate, various temperatures and cylinder pressures collected via a Microstar DAP, sampling at fast sampling rate and exhaust emissions data from the emission system sampling at low sampling rate. The cylinder pressure data acquisition was controlled by an encoder connected to the crank shaft of the engine. A sample was taken at every encoder pulse, i.e., every 0.2 crank angle degree. The cylinder pressure data was sampled by a Microstar 5400A/627 data acquisition processor. As soon as one cylinder passed exhaust valve opening, pressure and ion current data were transferred from the AD card to the control program. When a new pressure and ion current curve was available in the control program, a simplified rate of heat release calculation based on pressure and calculation of 50% of the ion current rise was performed where control inputs such as combustion timing ($\alpha_{50,p}$ and $\alpha_{50,ion}$), peak pressure and pressure gradient were sent to the controller. By changing the controllers mode the operator could switch between controlling by using $\alpha_{50,p}$ or $\alpha_{50,ion}$ as feedback of the combustion timing. The control signal, i.e., the output from Simulink controller, was then sent back to the main control program and the fuel injector was programmed with a new fuel setting. The two fuels have different autoignition temperatures, a property that was used to control the combustion timing. The fuel injection cycle begins at the top dead center gas exchange point (TDC_{GE}). In order to have cycle-to-cycle control, the inject duration was determined and programmed prior to TDC_{GE}. Conditional upon limits for cylinder peak pressure and pressure gradient, the control program had an engine check feature that will cut the fuel injection. The controller was implemented using Simulink and converted to C-code using the automatic code generation tool of Real Time Workshop.

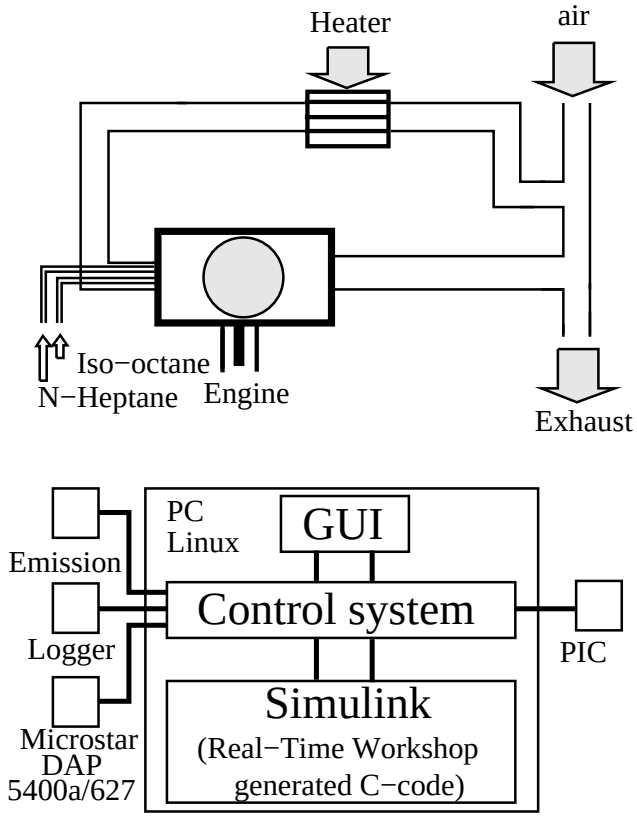

Fig. 1. Experimental set-up

Then, the C-code was compiled to an executable program communicating with the main control program. This gave us a system where controllers were easily implemented and put in operation, and the feature of being able to replace the existing controller, without restarting the system.

C. Ion current sensing system

A conventional spark plug, mounted in the center position of the head, was used as an ion current sensor. Figure 2 shows the principal layout of the measuring system. A DC voltage (U) of 85 V was applied across the electrode gap. The ion current was sampled by measuring the voltage over a resistance (R) of 100 kΩ, inserted in the electrical circuit. Since the signal level was low, in the order of a μA or lower, it was amplified before the A/D conversion was made. The amplifier had a gain of 23 and a bandwidth of 330 kHz.

III. COMPARISON BETWEEN CA50 BASED ON HEAT RELEASE AND ON ION CURRENT

Figure 3 shows a single cycle of ion current and heat release. Note that the ion current rise time and heat release coincide. Another characteristic is that there is heat release before the appearance of any ion current. This suggests that ion current measurement is local.

A. Combustion timing information in ion current data

The most distinct feature of the ion current trace seems to be the leading edge, as can be seen in Fig. 4. The idea here is

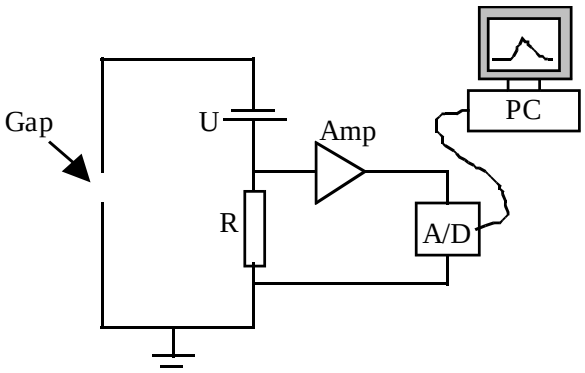

Fig. 2. Schematics of the ion current measuring system.

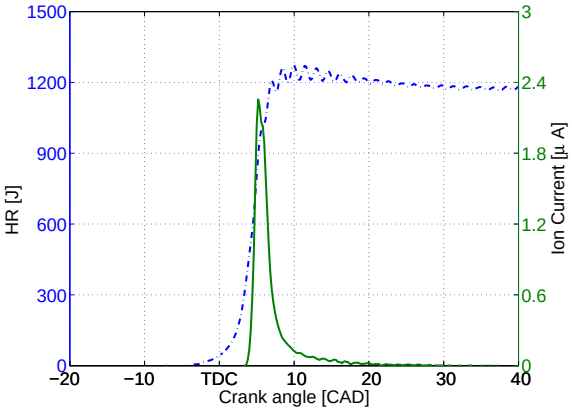

Fig. 3. Ion current (*solid*) and heat release (*dashed-dotted*) for a single cycle.

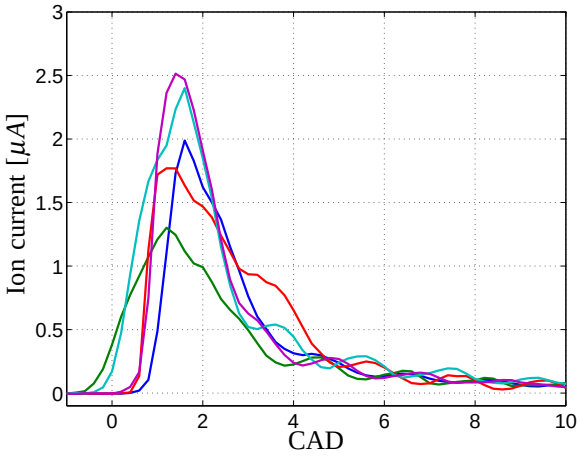

Fig. 4. Ion current from five consecutive cycles. Notice that the cycles has a spread in amplitude. The spread in timing is correlated to $\alpha_{50,p}$.

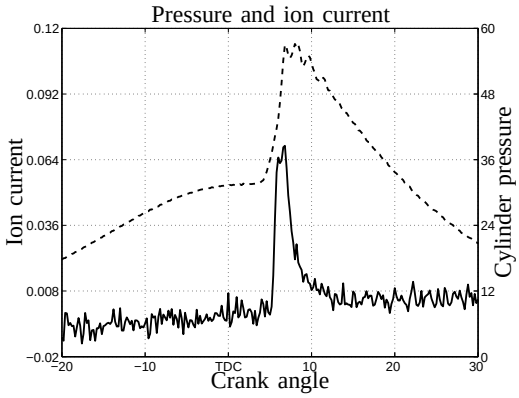

Fig. 5. Ion current (*solid*) and cylinder pressure (*dashed*).

to use this flank to detect combustion timing. The midpoint of this flank is designated $\alpha_{50,ion}$. Fig. 5 shows ion current and cylinder pressure for one engine cycle. Note that the ion current rising flank corresponds to the cylinder pressure increase due to the combustion. $\alpha_{50,p}$ being estimated by finding the CAD value where the heat release, based on pressure measurements, had reached half of it's maximum. Figure 6 shows the correlation is a bit more centered along the unity line. The cases noted '+' and 'x' both has a correlation coefficient of 0.87. The experiments was carried out in open loop. The coefficient of variance of Indicated Mean Effective Pressure (IMEP) for the '+' case was 2.31% and for the 'x' case was 1.59%. The autospectrum of $\alpha_{50,ion}$ and $\alpha_{50,p}$ is shown in Fig. 6. The coherence spectrum between $\alpha_{50,ion}$ and $\alpha_{50,p}$ is fairly close to one for several frequencies, suggesting that a linear relationship between $\alpha_{50,ion}$ and $\alpha_{50,p}$ might exist (Fig. 6).

IV. CONTROL BASED ON $\alpha_{50,ion}$ VERSUS $\alpha_{50,p}$

The PID controller was manually tuned and the parameters were the same for the two different feedback cases and no feedforward was present The control system response, when using feedback from ion current measurements ($\alpha_{50,ion}$) to step changes is shown in Fig. 7 and

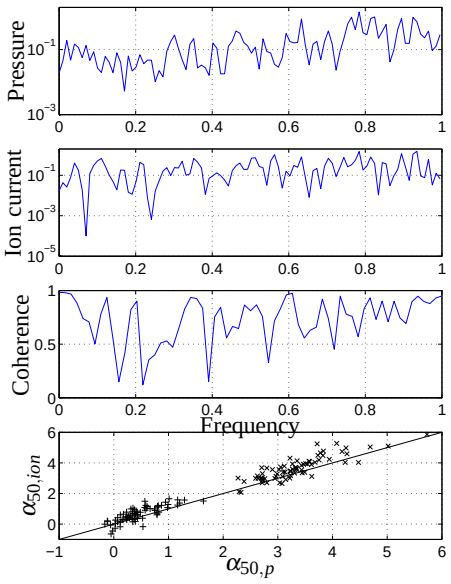

Fig. 6. Autospectrum of $\alpha_{50,p}$ (*upper*) and $\alpha_{50,ion}$ (*middle*). Coherence spectrum between $\alpha_{50,ion}$ and $\alpha_{50,p}$ (*middle*). Correlation between $\alpha_{50,ion}$ and $\alpha_{50,p}$. Two cases, 'x' and '+' (*lower*).

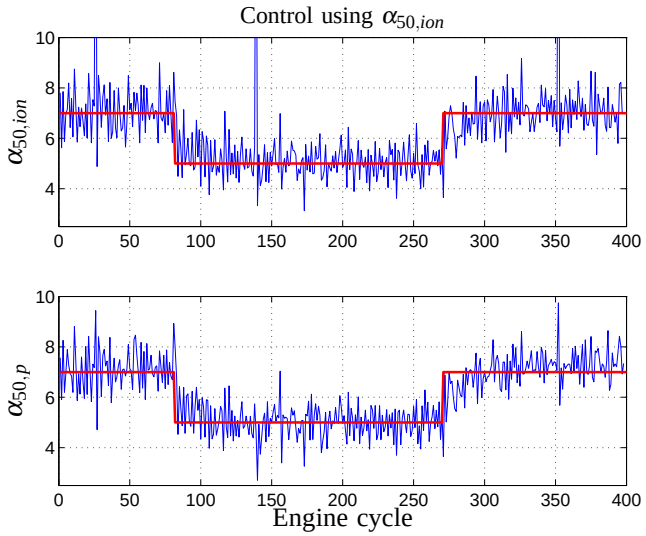

Fig. 7. CA50 step response when using $\alpha_{50,ion}$ as feedback (*upper*) and corresponding $\alpha_{50,p}$ (*lower*). The thick line is the reference value.

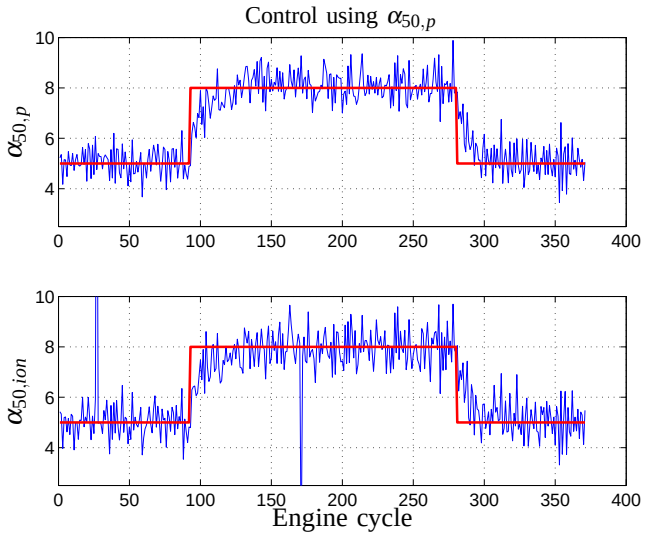

Fig. 8. CA50 step response when using $\alpha_{50,p}$ as feedback (*upper*) and corresponding $\alpha_{50,ion}$ (*lower*). The thick line is the reference value.

the corresponding $\alpha_{50,p}$ during the step change. The three outliers, cycle number 38, 140 and 363, in Fig. 7 were due to early detection problems of late combustion in the algorithm for estimation of $\alpha_{50,ion}$. Later examination of the ion current signal at these three outliers showed that the ion current signal was significant and detectable. Both cylinder pressure and ion current were measured simultaneously. Figure 8 shows the step response where feedback from pressure sensors ($\alpha_{50,p}$) was used and the corresponding $\alpha_{50,ion}$ during the step response. Also in this case later examination of the outliers at cycle number 28 and 180 showed that a better tuned algorithm could detect $\alpha_{50,ion}$. The step responses were performed at the same operating point of 3 bar net IMEP, an inlet temperature of 150°C, an engine speed of 1000 rpm and no EGR. The closed-loop control based on ion current gave good results with similar performance as the closed-loop control based on cylinder pressure sensor. In this experiment, the standard deviation of the CA50 estimation at constant CA50 set point was 0.65 CAD for $\alpha_{50,ion}$ and 0.56 CAD for $\alpha_{50,p}$. This corresponds to previous studies which shown $\alpha_{50,ion}$ and $\alpha_{50,p}$ give very similar results [5].

In Fig. 9, the distribution of the residuals is shown when controlling using $\alpha_{50,ion}$ and when using $\alpha_{50,p}$. As desired when using $\alpha_{50,ion}$ as feedback, we note that the residual distribution for $\alpha_{50,ion}$ was similar to normal distribution with zero mean. The corresponding residuals for $\alpha_{50,p}$ had an offset. When using $\alpha_{50,p}$ as feedback, the residual distribution for $\alpha_{50,p}$ was similar to normal distribution with zero mean and the corresponding residuals for $\alpha_{50,ion}$ had an offset similar to the case when controlled by $\alpha_{50,ion}$ The resulting autocorrelation of the control error, when using $\alpha_{50,ion}$, had residuals approximately independent. This was also the case when controlling using $\alpha_{50,p}$.

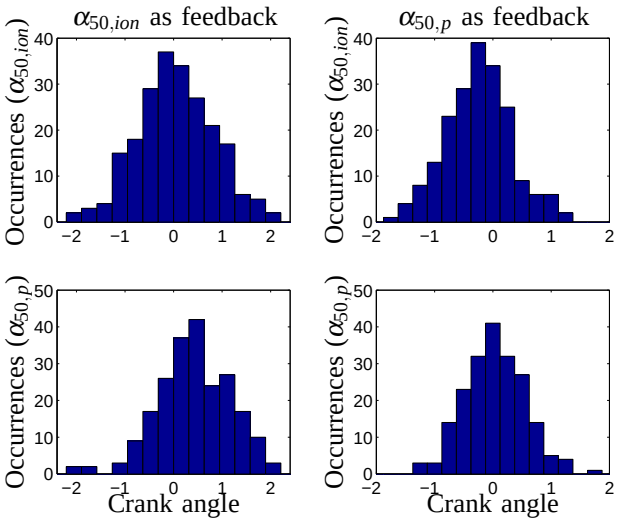

Fig. 9. The distribution of the residuals when controlling by CA50 based on ion current (*left*). The residual distribution of $\alpha_{50,ion}$ (*upper left*) and $\alpha_{50,p}$ (*lower left*). The distribution of the residuals when controlling by CA50 based on pressure (*right*). The residual distribution of $\alpha_{50,ion}$ (*upper right*) and $\alpha_{50,p}$ (*lower right*).

V. Identification and Modeling

Whereas the signals representing ion current and pressure signal are intimately related, they are not identical. A Bode diagram representing the transfer function from ion current to pressure is given in Fig. 10, and in Fig. 11 the simulated model output together with measured output is presented. The transfer functions have been identified by estimating ARMAX models [2]. The resulting continuous-time model

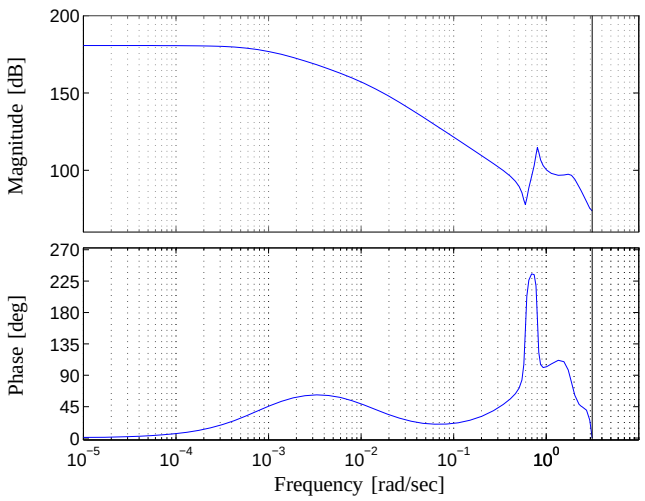

Fig. 10. Bode diagram of the transfer function between ion current measurement without side electrode and pressure. Ion current is input and pressure is the output of the 6:th order ARMAX model.

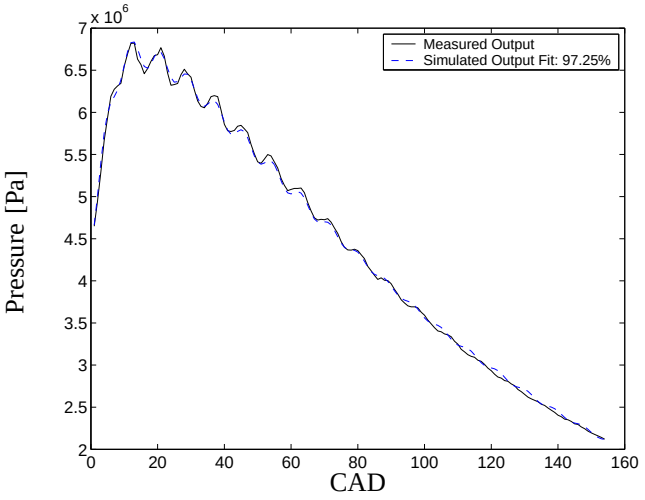

Fig. 11. The simulated model pressure output (*dashed*) together with measured pressure (*solid*). Model used being the same as in Fig. 10.

written in transfer function form is

$$G(s) = \frac{B(s)}{A(s)}$$

$$A(s) = s^4 + 1880s^3 + 7.03\cdot10^8 s^2 + 5.45\cdot10^{11}s + 1.06\cdot10^{14}$$

$$B(s) = 6630s^4 + 1.36\cdot10^9 s^3 + 9.23\cdot10^{13}s^2 + 2.07\cdot10^{18}s - 1.16\cdot10^{21}$$

Since model-based control design have many benefits, models which had $\alpha_{50,ion}$ and $\alpha_{50,p}$ as output were estimated. An HCCI is a MIMO system, but in the estimation of models suitable for combustion timing control design only $\alpha_{50,ion}$ was used as output, since the signal is a reliable indication of the combustion. The input to the process was the fuel ratio, $IMEP_{net}$. Pre-processing of the data, removal of offsets and/or trends were performed before

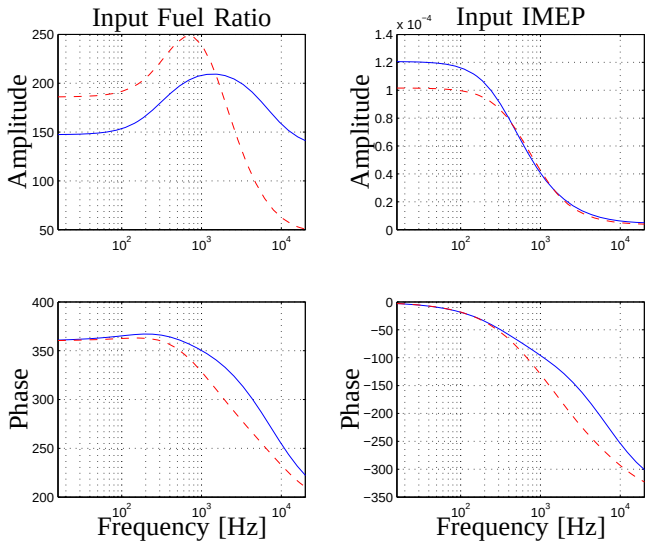

Fig. 12. Bode diagram (*left*) showing the transfer function from fuel ratio to $\alpha_{50,ion}$ (*solid*) and $\alpha_{50,p}$ (*dashed*). Bode diagram (*right*) showing the transfer function from IMEP to $\alpha_{50,ion}$ (*solid*) and $\alpha_{50,p}$ (*dashed*).

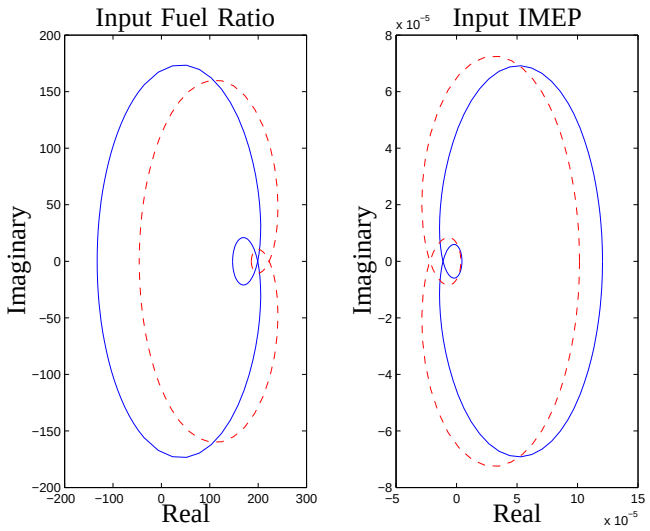

Fig. 13. Nyquist diagram (*left*) from fuel ratio to $\alpha_{50,ion}$ (*solid*) and $\alpha_{50,p}$ (*dashed*). Nyquist diagram (*right*) showing from IMEP to $\alpha_{50,ion}$ (*solid*) and $\alpha_{50,p}$ (*dashed*).

the identification procedure started. Linear models have been identified by using sub space-based methods [7]. The identification results indicated that a second-order model was sufficient, and Fig. 12 shows the Bode diagram of the second-order models from fuel ratio and $IMEP_{net}$ to $\alpha_{50,ion}$ and $\alpha_{50,p}$. The Nyquist curve of the second order models from fuel ratio and $IMEP_{net}$ to $\alpha_{50,ion}$ and $\alpha_{50,p}$ is shown in Fig. 13. Figure 14 shows 3-step ahead predicted model output of the two identified models. As can be noted, the model predicts the output well. Residual analysis has also been performed with good results. Figure 15 shows the sensitivity functions for the transfer functions from fuel

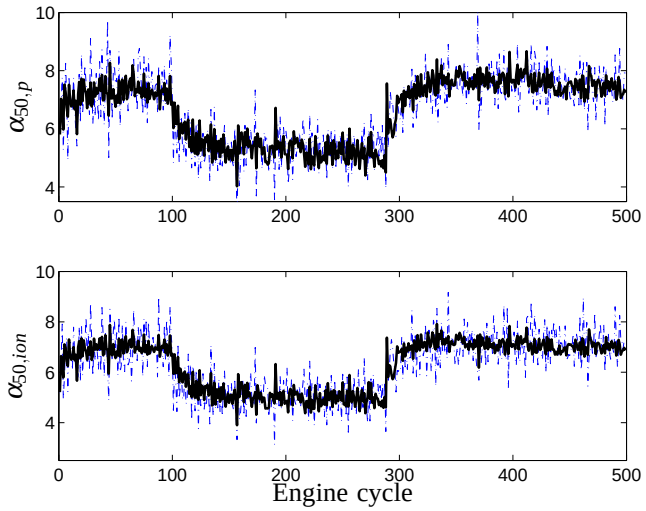

Fig. 14. Responce in $\alpha_{50,p}$ and $\alpha_{50,ion}$ to step changes in CA50 reference. Upper figure: 3-step ahead predicted model output (*black*) and $\alpha_{50,p}$ (*grey*). Lower figure: 3-step ahead predicted model output (*black*) and $\alpha_{50,ion}$ (*grey*)

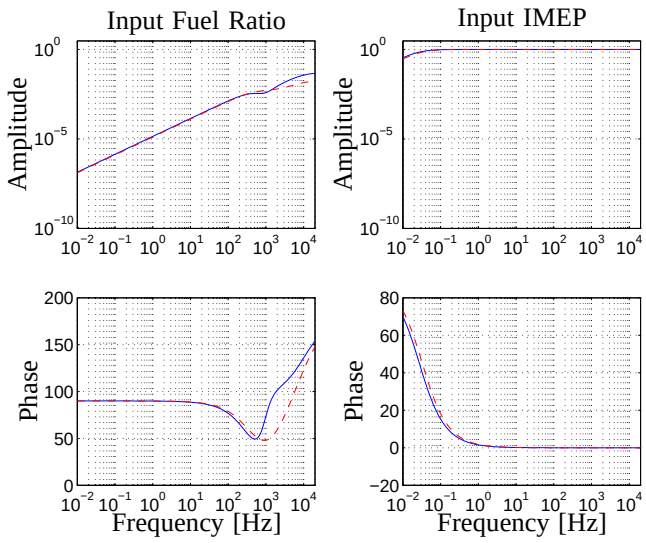

Fig. 15. Sensitivity functions for the transfer functions from fuel ratio and IMEP to $\alpha_{50,p}$ (*grey*) and $\alpha_{50,p}$ (*black*), respectively.

ratio and IMEP to $\alpha_{50,p}$ and $\alpha_{50,p}$.

VI. Discussion

This paper is a continuation of the work presented in [6]. The clearcut relationship between cylinder pressure and ion current measurement suggests that one measurement may be reconstructed from the other for instance by means of a Kalman filter or some other full-order observer. Apparently, cylinder pressure measurements provide a more robust CA50 estimation than ion current measurements. In this experimental set-up, the upper limit of λ-value (relative air/fuel ratio) seems to be 2.7 for a reliable ion current signal. At higher λ-values, the noise level corrupts the measurements. However, in another experimental set-up with lower compression ratio, a lower upper limit has been found [5]. The rich limit for HCCI operation is λ=2.

Questions not yet fully addressed are what is the limit of operating conditions, and whether the ion current measurements could replace pressure sensors in a production-like environment.

A remark on using IMEP as an input, is that it is not independent of the fuel ratio, since the efficiency is dependent on CA50. It is obvious that the controlled variables have a significant perturbation which appears to be of a stochastic nature. Early investigation by simulation suggests that stochastic control strategies, such as minimum variance control based on pressure or ion current, seem to give no significient improvement of the output variance as compared to PID control.

VII. Conclusion

Controlling a HCCI engine by using ion current measurements was found to work well for a range of λ of $[2, 2.7]$. CA50 based on ion current measurement and CA50 based on calculated heat release using cylinder pressure gave similar results and hence the performance for the case of ion current was similar to the case where pressure sensors were used. In this experimental set-up it was found that the upper limit of the λ-value (relative air/fuel ratio) was 2.7 for a reliable ion current signal.

References

[1] A. Franke. *Characterization of an Electrical Sensor for Combustion Diagnostics*. PhD thesis, Lund Institute of Technology, ISRN LUTFD/TFCP–80–SE, 2002.

[2] R. Johansson. *System Modeling and Identification*. Prentice Hall, Englewood Cliffs, New Jersey, 1993.

[3] J-O Olsson, P Tunestål, and B. Johansson. Closed-Loop Control of an HCCI engine. In *SAE 2001-01-1031*.

[4] R. Reinmann. *Theoretical and Experimental Studies of the Formation of Ionized Gases in Spark Ignition Engines*. PhD thesis, Lund Institute of Technology, ISBN 91-628-2985-8, 1998.

[5] P. Strandh, J. Bengtsson, M. Christensen, R. Johansson, A. Vressner, P. Tunestål, and B. Johansson. Ion current sensing for HCCI combustion feedback. In *SAE Technical Paper 2003-01-3216*, 2003.

[6] P. Strandh, J. Bengtsson, R. Johansson, P. Tunestål., and B. Johansson. Cycle-to-cycle control of a dual-fuel HCCI engine. In *SAE Technical Paper 2004-01-0941*, 2004.

[7] M. Verhaegen. Identification of the deterministic part of MIMO state space models. *Automatica*, 30:61–74, 1994.